SUMER OBSERVATIONS OF SOLAR TRANSITION REGION STRUCTURES AND DYNAMICS

Ingolf E. Dammasch, [1] and Klaus Wilhelm[1]

[1]*Max-Planck-Institut für Aeronomie, Max-Planck-Straße 2, D-37191 Katlenburg-Lindau, Germany*

ABSTRACT

Several raster scans of the UV/EUV spectrometer SUMER (Solar Ultraviolet Measurements of Emitted Radiation) on SOHO (the Solar and Heliospheric Observatory of ESA and NASA) in quiet-Sun regions were used to study the region between the chromosphere and the corona, i.e., the transition region with a temperature range between $\approx 30\,000$ K and $400\,000$ K. A typical SUMER scan of 100 raster steps with the $300''$-long slit leads to 30 000 pixels containing spectral information and it is, therefore, a good statistical base. The aim was to calculate probability distributions of line intensities and shifts, and to study the relationship between intensities and shifts. These signatures were determined for emission lines with various formation temperatures across the transition region. Results show that intensity contrasts as well as Doppler shifts depend on the formation temperature and peak around 100 000 K, which is also the region with the strongest relation between line intensities and shifts.

INTRODUCTION

The chromospheric network of quiet-Sun (and coronal hole) regions is a prominent feature in all UV/EUV emission lines from the transition region with formation temperatures between several ten thousand and several hundred thousand kelvin. The network lanes display a significant amount of variability both in line intensities and in Doppler shifts. The line shifts we will interpret as bulk motions of the plasma, if the emitting medium can be considered to be optically thin. An understanding of the structure and the dynamics of the chromospheric network is of considerable interest as the sources of the solar wind have been found within the network lanes (Hassler et al., 1999), and the energy supply for heating the solar corona in all likelihood has to be funnelled through the lanes as well. Figure 1 shows a quiet-Sun region with the chromospheric network at different temperatures. The obvious differences in contrast will be quantified by examining the intensity distributions.

SUMER observations will be used to study in detail some of the statistical properties of the radiation from the transition region, extending earlier observations of this type (Skumanich et al., 1975; Reeves, 1976; Wilhelm et al., 1998; Griffiths et al., 1999; Dammasch et al., 1999a). The relationship between line intensity and Doppler shifts has been investigated by Brynildsen et al. (1998).

DATA SELECTION AND ANALYSIS

Two groups of SUMER studies were selected and treated separately: scans with long exposure times ranging from 90 s to 150 s per raster step, and those with short exposure times around 15 s. Most of the scans were taken in 1996 and 1999, but both groups also include studies from 1997/98, which use the solar rotation instead of raster steps.

The observations to be analysed were selected in such a way that they only cover quiet-Sun regions. Scans including active regions, filaments, coronal holes or the solar limb were not taken into consideration for this study, because their intensities and Doppler shifts follow individual distributions that are not generally comparable, i.e., only QS data generally follow log-normal distribution as discussed below. An active region has been discussed by Griffiths et al. (2000), who also found different distributions for quiet-Sun and active regions. Here we consider altogether eleven studies including 26 different lines in the first group with long

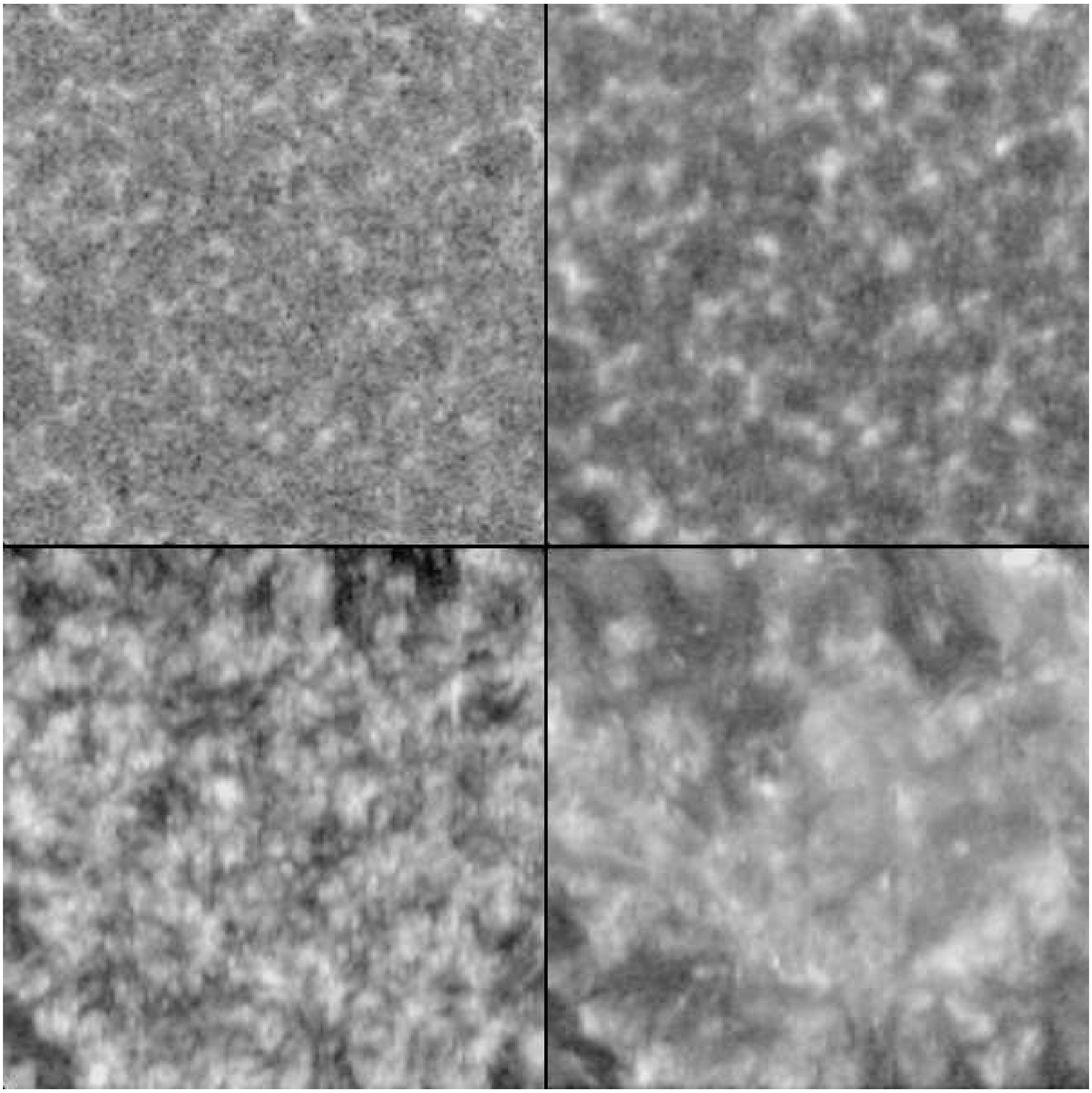

Fig. 1. Morphological structure of the solar atmosphere at different temperatures, represented by the lines C I, Si II, N IV, and Ne VIII. The examples are taken from a SUMER raster scan of 7 November 1999. The same area of $300'' \times 300''$ is covered in each of the frames. The brightness is shown on a logarithmic scale.

exposure times. In the second group, 22 studies including 31 different lines were used with short exposure times.

An attempt was made to cover the formation temperature range between 10 000 K and 1 000 000 K, and especially the transition region, as completely as possible. Lines with insufficient intensities had to be excluded, or at least not all their results could be considered, due to bad signal-to-noise ratios and resulting low-quality fits. Nevertheless, even the reliable lines still cover a wide intensity range (a factor of 100 between the highest and lowest values). It cannot be ruled out that this may have an influence on the probability distributions by introducing a widening of the distributions for small signal-to-noise ratios. - Another influence on the distributions is spatial binning: in the intercalibration study of 2 November 1999, the N V scan and the Mg X scans were binned (three spatial pixels). According to simulation studies, this leads to approximately 10 % narrower probability distributions, which was subsequently corrected.

The data were treated with the standard SUMER software to correct for detector local-gain and deadtime effects. Detector sensitivity, geometric distortion and thermoelastic effects were corrected with methods described elsewhere (Dammasch et al., 1999b). For each $1''$-pixel scanned on the solar surface, the line profile was treated individually: the continuum intensity level was estimated and subtracted, the remaining line intensity was integrated and the line position determined using methods described by Dammasch et al. (1999b). Doppler shifts were calculated relative to the average line position of the whole scan. This selection has no influence on the width of the distribution.

The logarithms of line and continuum intensities were calculated and grouped into 60 bins of size 0.1, covering 0.01 to 10 000 count s^{-1} $arcsec^{-2}$ $line^{-1}$ or $Å^{-1}$, respectively. Doppler shifts were grouped into 60 bins of size 1 km s^{-1}, covering $\pm$ 30 km s^{-1}. The resulting probabilities were fitted to a Gaussian distribution $p(x) = a\ \exp(-(\mathrm{x}-\mu)^2/(2\sigma^2))$, where x denotes bin 1, ..., 60. The parameter that describes the variability of intensity or Doppler shift is the standard deviation, σ.

To describe the relation between line intensity and line shift, the pixels were sorted according to intensity, grouped into approximately 30 bins of 1 000 pixels each, and their shifts averaged per bin. The bins were scaled between 0 and 1 and a linear fit was calculated for the average shifts. The parameter that describes the relationship between intensity and shift is the slope: an increase in intensity either leads to a redshift (positive slope) or a blueshift (negative slope).

Resulting values for these four signatures (width of line intensity distribution, width of continuum intensity distribution, width of line shift distribution, slope of average shift vs. scaled intensity) can be found in Figures 3, 4, 6, and 7.

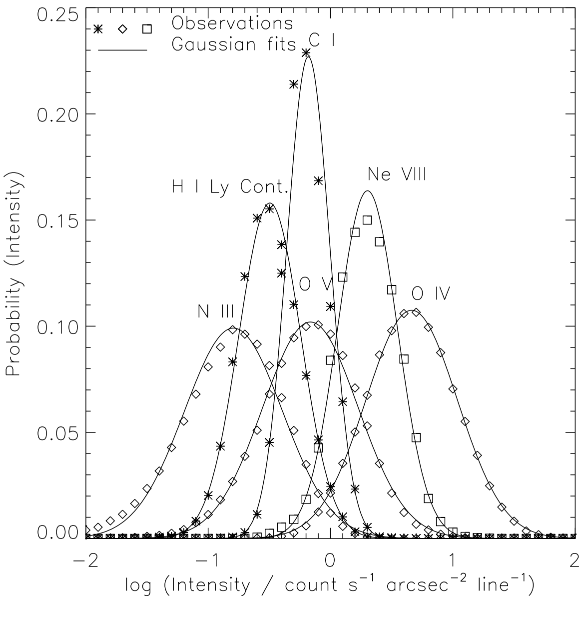

Fig. 2. Probabilities of logarithms of intensities fitted to normal distributions. Most examples are taken from a SUMER study in June 1998, C I is from February 1999.

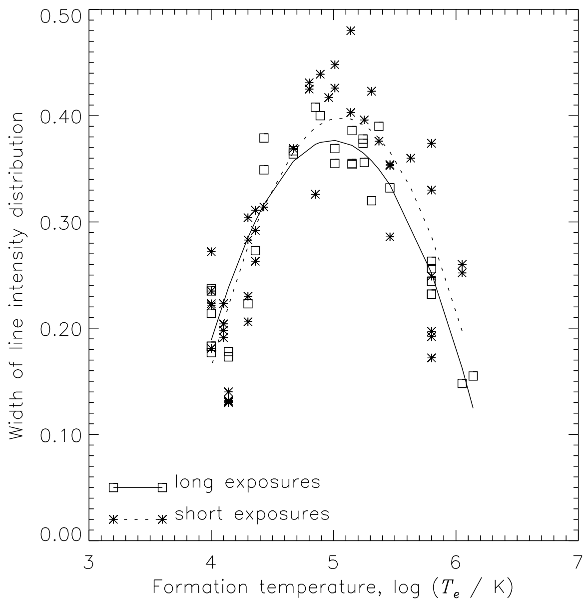

Fig. 3. Widths of log-normal probability distributions of line intensities vs. line formation temperatures. The unit of the width is the same as shown in Figure 2, i.e., log (intensity/count s^{-1} $arcsec^{-2}$ $line^{-1}$). Widths are measured by the standard deviation, σ, of the Gaussian fits.

RESULTS AND DISCUSSION

(1) The logarithms of the intensities can generally be fitted with a Gaussian probability distribution quite well. This is in accordance with Pauluhn et al. (2000), who also tried other distribution types, and considered the log-normal distribution to be the optimal choice (Figure 2).

(2) The widths of the log-normal probability distributions show a dependence on the formation temperature: they start with their narrowest values in the chromosphere, peak at twice this width in the transition region around 100 000 K, and almost return to their initial values in the corona. While the chromospheric values do not appear to be influenced by the exposure time, transition-region and coronal values are generally higher for short exposure times. This points to intensity variations on short time scales that may be averaged during minute-long exposure times, thus leading to narrower probability distributions (Figure 3). The large variation at $\log(T_e/\mathrm{K}) = 5.8$ is due to the Ne VIII line, which shows a potential for very different structures (network-related as well as homogeneously cloud-like) and resulting distributions.

(3) The continua observed in our spectral range behave like lines being formed around 10 000 K. They show distribution widths typical for this temperature, and a wavelength dependence characterized by a drop in width from 700 Å to 1500 Å, best to be observed for long exposure times (Figure 4). When compared to the fitted relationship in Figure 3, the widths suggest a temperature drop from ≈ 16 000 K (for the 700-Å continuum) to ≈ 8 000 K (for the 1500-Å continuum). This correlates with a different morphological structure, as demonstrated in Figure 5.

(4) The widths of the line shift probability distributions also show a temperature dependence. They start with low values in the chromosphere and reach their highest values in the transition region just above 100 000 K. In the corona they seem to drop again (although not quite back to chromospheric values), which is best observed for long exposure times (Figure 6).

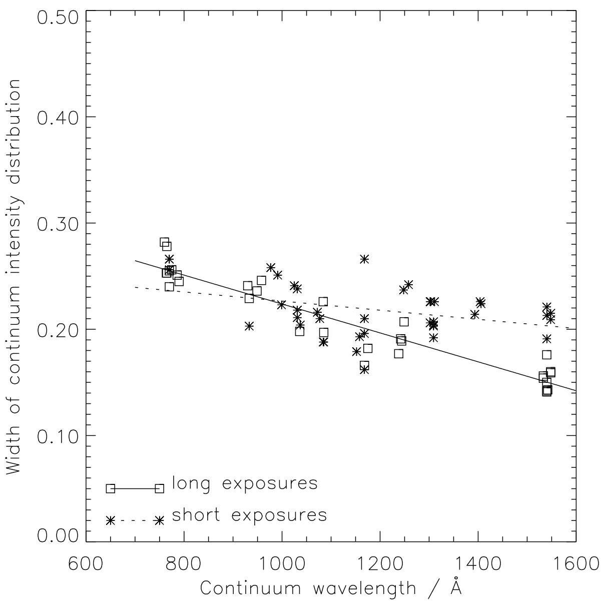

Fig. 4. Widths of log-normal probability distributions of continua intensities vs. continua wavelengths. For the unit of the width see Figure 3.

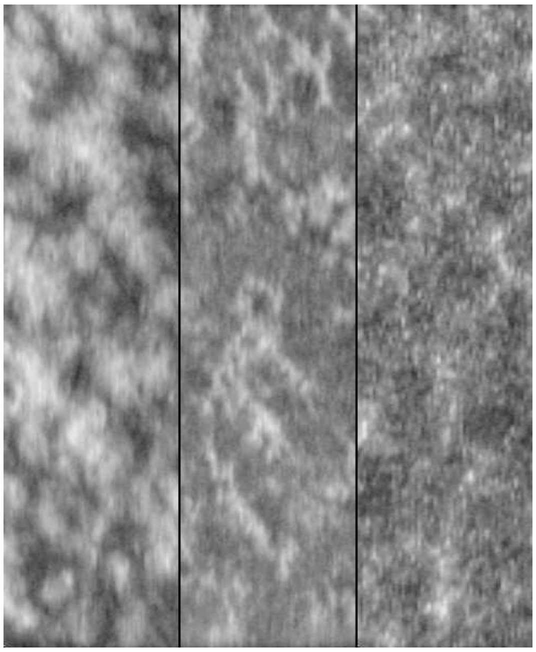

Fig. 5. Morphological structure of continua at wavelengths of 700 Å, 1 100 Å, and 1500 Å corresponding predominantly to the H I Lyman, C I and the thermal continua. The examples are taken from SUMER raster scans of different quiet-Sun regions in February and March 1999. The area covered is 81″ × 300″ in each case. Brightness is shown on a logarithmic scale.

(5) The relationship between average line shift and intensity can best be observed for short exposure times. With the exception of Si II 1309 Å, which appears to have a non-Gaussian line profile and shows a negative slope, the low-chromospheric lines start with a flat slope. Upper-chromospheric and transition-region lines show increasing positive slopes, i.e., red shifts for high intensities. The dependence again peaks around 100 000 K. The values for coronal lines go back to zero and sometimes below, which would then indicate blueshifts for high intensities in quiet-Sun regions (Figure 7).

These results confirm earlier findings using a smaller number of lines (Wilhelm et al., 1998; Dammasch et al., 1999a) and are in good agreement with independent studies (Griffiths et al., 1999; Pauluhn et al., 2000). Bogdan et al. (1988) discuss magnetic fragmentation processes as a possible source for log-normal distributions. The results are in line with studies on the contrast between network/cell boundaries and interior performed with the SUMER instrument (Feldman et al., 2000) and earlier instruments (Feldman et al., 1976; Reeves, 1976), which also point to an increase in intensity contrast for transition region lines with a maximum near 100 000 K.

It should be mentioned that the temperature interval of highest red shifts observed by other authors (Doschek et al., 1976; Brekke et al., 1997; Chae et al., 1998; Peter and Judge, 1999) coincides with the temperature where we find the greatest dynamical range. Explosive events (cf., e.g., Dere et al., 1989; Innes et al., 1997) are also most pronounced in this temperature range. They are thought to be the direct consequence of magnetic reconnection activity and could be the initial process of a chain of events leading to the observed temperature dependence of many parameters in the transition region.

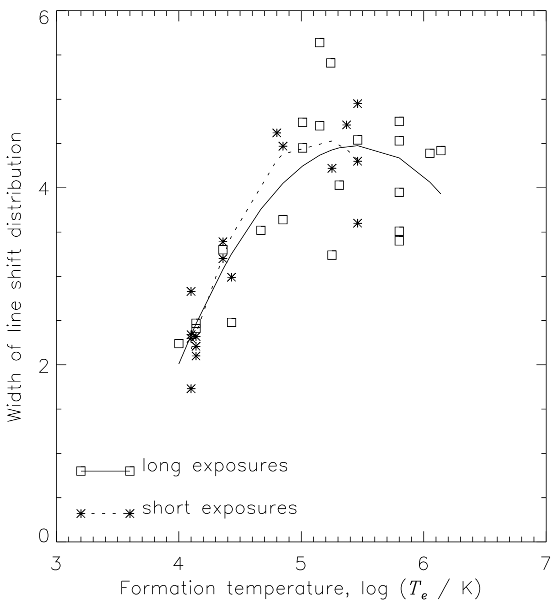

Fig. 6. Widths of normal probability distributions of line shifts vs. line formation temperatures. The unit of the width is kilometre per second.

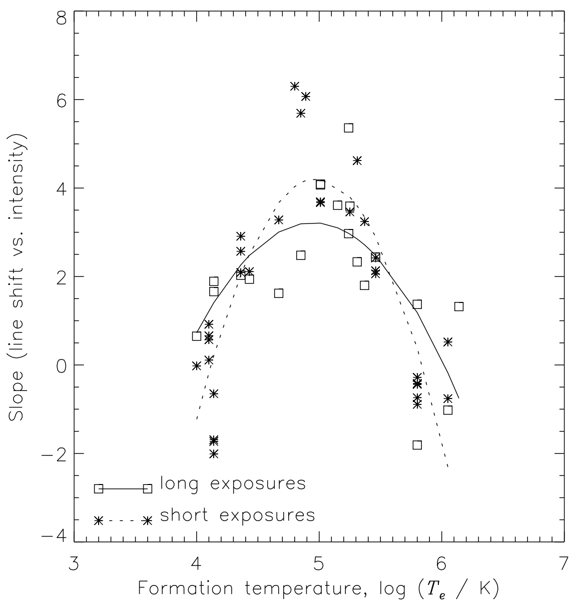

Fig. 7. Relations between average line shifts and line intensities vs. line formation temperatures. The average line shift is measured in kilometre per second, the intensity is scaled between 0 and 1, i.e., the slope is identical to the velocity difference between the darkest and the brightest pixels.

ACKNOWLEDGEMENTS

SUMER is financially supported by DLR, CNES, NASA and the ESA PRODEX programme (Swiss contribution). SOHO is a project of international co-operation between ESA and NASA.

REFERENCES

Bogdan, T. J., P. A. Gilman, I. Lerche, and R. Howard, Distribution of Sunspot Umbral Areas: 1917–1982, *Astrophys. J.*, **327**, 451-456, 1988.

Brekke P., D. M. Hassler, and K. Wilhelm, Doppler Shifts in the Quiet-Sun Transition Region and Corona Observed with SUMER on SOHO, *Solar Phys.*, **175**, 349-374, 1997.

Brynildsen, N., P. Brekke, T. Fredvik, S. V. H. Haugan, O. Kjeldseth-Moe, et al., SOHO Observations of the Connection between Line Profile Parameters in Active and Quiet Regions and the Net Red Shift in EUV Emission Lines, *Solar Phys.*, **181**, 23-50, 1998.

Chae, J., H. S. Yun, and A. I. Poland, Temperature Dependence of Ultraviolet Line Average Doppler Shifts in the Quiet Sun, *Astrophys. J. Suppl. Ser.*, **114**, 151-164, 1998.

Dammasch, I. E., D. M. Hassler, W. Curdt, and K. Wilhelm, Statistical Analysis of EUV Lines Inside and Outside of Solar Coronal Holes, *Space Sci. Rev.*, **87**, 161-164, 1999a.

Dammasch, I. E., K. Wilhelm, W. Curdt, and D. M. Hassler, The Ne VIII (λ770) Resonance Line: Solar Wavelengths Determined by SUMER on SOHO, *Astron. Astrophys.*, **346**, 285-294, 1999b.

Dere, K. P., J.-D. F. Bartoe, and G. E. Brueckner, Explosive Events in the Solar Transition Zone, *Solar Phys.*, **123**, 41-68, 1989.

Doschek, G. A., U. Feldman, and J. D. Bohlin, Doppler Wavelength Shifts of Transition Zone Lines Measured in SKYLAB Solar Spectra, *Astrophys. J.*, **205**, L177-L180, 1976.

Feldman, U., G. A. Doschek, and N. P. Patterson, The Quiet Sun Chromospheric Network Observed from SKYLAB, *Astrophys. J.*, **209**, 270-281, 1976.

Feldman, U. , I. E. Dammasch, and K. Wilhelm, The Morphology of the Solar Upper Atmosphere During the Sunspot Minimum, *Space Sci. Rev.*, **93**, 411-472, 2000.

Griffiths, N. W., G. H. Fisher, D. T. Woods, and O. H. W. Siegmund, SUMER Observations of the Quiet-Sun Transition Region, *Astrophys. J.*, **512**, 992-1005, 1999.

Griffiths, N. W., G. H. Fisher, D. T. Woods, L. W. Acton, and O. H. W. Siegmund, Simultaneous SOHO and YOHKOH Observations of a Small Solar Active Region, *Astrophys. J.*, **537**, 481-494, 2000.

Hassler, D. M., I. E. Dammasch, P. Lemaire, P. Brekke, W. Curdt, et al., Solar Wind Outflow and the Chromospheric Magnetic Network, *Science*, **283**, 810-813, 1999.

Innes, D. E., B. Inhester, W. I. Axford, and K. Wilhelm, Bi-directional Plasma Jets Produced by Magnetic Reconnection on the Sun, *Nature*, **386**, 811-813, 1997.

Pauluhn, A., S. K. Solanki, I. Rüedi, E. Landi, and U. Schühle, Statistics of Quiet Sun Extreme Ultraviolet Intensities, *Astron. Astrophys.*, **362**, 737-745, 2000.

Peter, H., and P. G. Judge, On the Doppler Shifts of Solar Ultraviolet Emission Lines, *Astrophys. J.*, **522**, 1148-1166, 1999.

Reeves, E. M., The EUV Chromospheric Network in the Quiet Sun, *Solar Phys.*, **46**, 53-72, 1976.

Skumanich, A., C. Smythe, and E. N. Frazier, On the Statistical Description of Inhomogeneities in the Quiet Solar Atmosphere, I. Linear Regression Analysis and Absolute Calibration of Multichannel Observations of the Ca^+ Emission Network, *Astrophys. J.*, **200**, 747-764, 1975.

Wilhelm, K., P. Lemaire, I. E. Dammasch, J. Hollandt, U. Schühle, et al., Solar Irradiances and Radiances of UV and EUV Lines During the Minimum of the Sunspot Activity in 1996, *Astron. Astrophys.*, **334**, 685-702, 1998.